Boundary-Layer Distortion on a Spinning Cone

WALTER B. STUREK*
U.S. Army Ballistic Research Laboratories, Aberdeen Proving Ground, Md.

Nomenclature

C_Y = Magnus (side) force coefficient, F_Y/qS
D = diameter of base of cone, 3.0625 in.
F_Y = side force
l = model length, 8.68 in.
p = spin rate, rad/sec
q = dynamic pressure, $\rho V^2/2$
Re_l = Reynolds number, $\rho Vl/\mu$
S = reference area, base of cone, $\pi D^2/4$
V = freestream velocity
α = angle of attack
μ = viscosity
ρ = density
ϕ = azimuthal angle, see Fig. 1
ω = spin rate, rpm

Introduction

THE Magnus force and its associated moment are usually small; however, their effects are important because they act to undamp the projectile throughout the flight. Theoretical analyses of the flow over a spinning body at angle of attack are not sufficiently general in application to be useful for design purposes. These analyses model the Magnus force as being caused by spin induced distortion of a fully laminar or fully turbulent boundary layer. The Magnus force calculated according to this model is very small. It has been suggested that a more critical case would be where transition of the boundary layer occurs on the body. In this case, spin induced distortion would affect the location of boundary-layer transition as well as the development of the boundary layer; and would presumably result in a much larger force.

Reported here are experimental data that show: 1) the effect of spin on boundary-layer transition, and 2) the effect of boundary-layer configuration on the measured Magnus force.

Spin Distortion of Boundary-Layer Transition

Normally, the flow along a model mounted in a wind tunnel is visible at only two locations on the model surface—the top and the bottom. Using an offset strut and rolling the model incrementally about the axis of the strut enables the entire surface of the model to be viewed. This technique has been applied to obtain spark shadowgraphs of the flow about the entire circumference of a 10° half-angle cone model. Shadowgraphs were taken at 15° increments in azimuth. Pictures were obtained both as the model spun down from a high spin rate and while the model was held at a constant spin rate. Figure 1 shows the coordinate system and sign convention used.

The location of boundary-layer transition completely about the circumference of the cone model was determined from the spark shadowgraphs. The position of transition was identified as

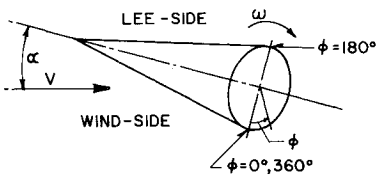

Fig. 1 Coordinate system.

Received August 7, 1972; presented as Paper 72-967 at AIAA 2nd Atmospheric Flight Mechanics Conference, Palo Alto, Calif., September 11–13, 1972; revision received October 16, 1972.

Index categories: Boundary-Layer Stability and Transition; Supersonic and Hypersonic Flow.

* Aerospace Engineer, Wind Tunnels Branch, EBL. Member AIAA.

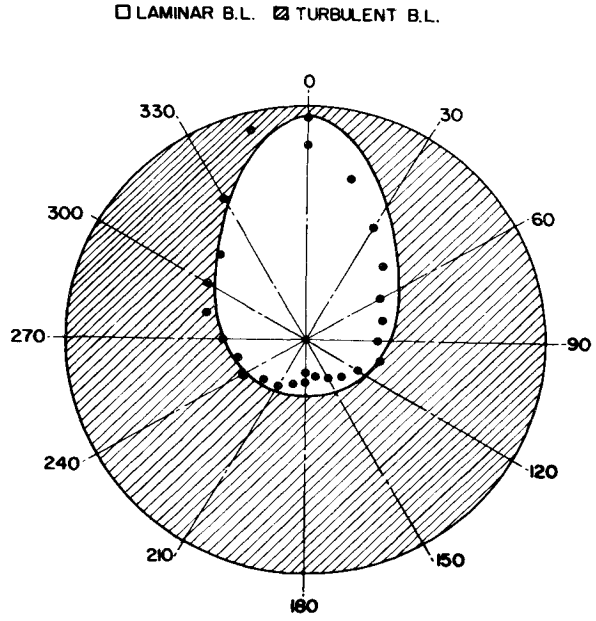

Fig. 2 Profile of boundary-layer transition about circumference of 10° cone, $M = 2$, $\alpha = 4°$, $Re_l = 5.97 \times 10^6$, $\omega = 0$.

the first indication of a change in the appearance of the laminar boundary layer. This criteria was used because it was easier to identify in the shadowgraphs than, say, the location of the boundary layer becoming fully turbulent. No attempt has been made to relate the location of boundary-layer transition determined as indicated above with that determined by other instrumentation.

An example of the transition data for zero spin, $M = 2$, $\alpha = 4°$, is shown in Fig. 2. The profile obtained with the model spinning at 20,000 rpm is shown in Fig. 3. In these figures, the distance from the center of the circle to the location of transition represents the distance on the cone from the tip of the cone along a ray to the location of boundary-layer transition. The profile of transition is seen to be displaced in azimuth in the same direction as the spin. The trends indicated are: 1) transition is delayed where the spin velocity is in the same direction as the cross-flow velocity, and 2) transition occurs sooner where the spin velocity opposes the cross-flow velocity.

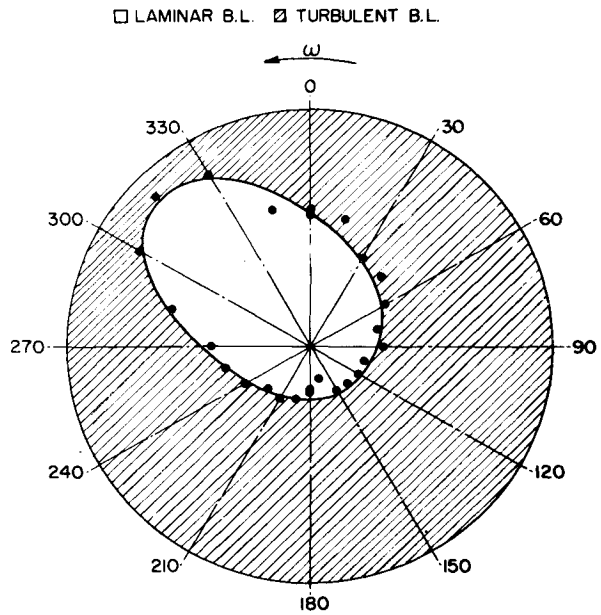

Fig. 3 Profile of boundary-layer transition about circumference of 10° cone, $M = 2$, $\alpha = 4°$, $Re_l = 5.97 \times 10^6$, $\omega = 20{,}000$ rpm, $pD/V = 0.31$.

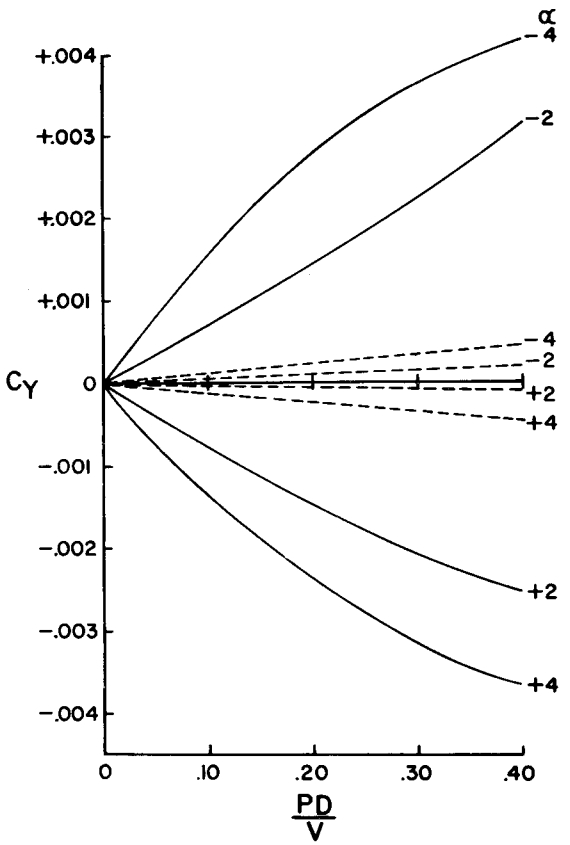

Fig. 4 Magnus force coefficient vs spin rate for cone model comparing measurements for transitional boundary layers:—$M = 2.0$, $Re_l = 1.80 \times 10^6$, laminar boundary layer on wind side, turbulent boundary layer on lee side -- $M = 2.0$, $Re_l = 6.0 \times 10^6$, natural transition to turbulent boundary layer on model surface.

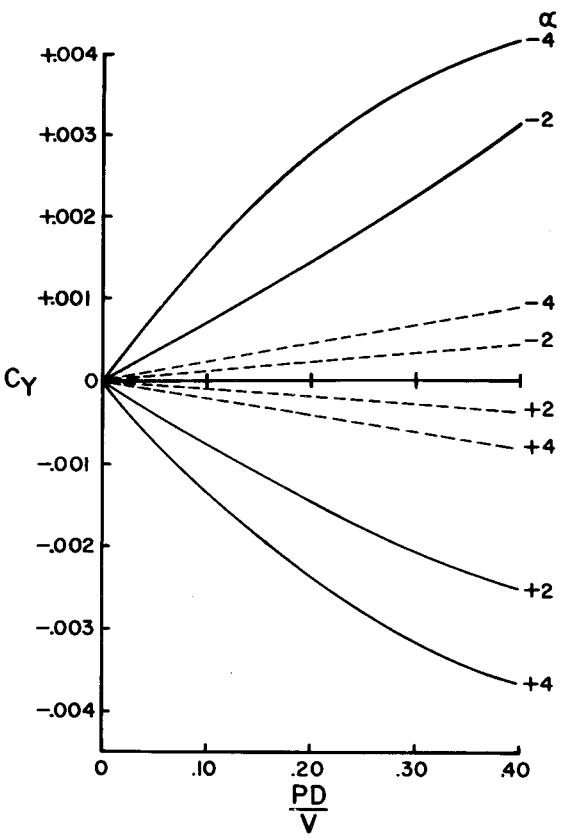

Fig. 5 Magnus force coefficient vs spin rate for cone model comparing measurements for transitional and tripped turbulent boundary layers:—$M = 2.0$, $Re_l = 1.80 \times 10^6$, laminar boundary-layer on wind side, turbulent boundary-layer on lee side; -- $M = 2.0$, $Re_l = 6.1 \times 10^6$, turbulent boundary-layer, boundary layer trip near tip of cone.

Force Measurements

Measurements of Magnus force have been obtained using the strain gage balance technique. Data have been obtained for tunnel operating conditions duplicating those for the spark shadowgraphs and, in addition, at lower values of tunnel total pressure to yield significantly different boundary-layer configurations on the model.

Data are compared in Fig. 4 for different boundary-layer configurations. The solid line represents data obtained at a low value of tunnel total pressure which resulted in the boundary layer on the wind-side remaining laminar at the base of the cone while transition to turbulence occurred on the lee-side near the tip of the cone. This resulted in a large difference in thickness of the boundary layer from the wind to the lee-side($\delta \approx 0.10$ in.: lee; $\delta \approx 0.02$ in.: wind). The broken line represents data obtained at a high value of tunnel total pressure for which natural transition to turbulence occurred completely about the model surface. It is seen that the configuration with the greatest difference in boundary-layer thickness from the wind to the lee-side results in the largest Magnus force. For the configurations shown, the Magnus force is changed by a factor of eight by a change in Reynolds number of only a factor of three.

In Fig. 5, a comparison similar to that in Fig. 4 is made. The comparison in Fig. 5 is between a boundary-layer tripped to turbulent by a sand strip placed 1 in. from the tip of the cone and a boundary layer which remained laminar on the wind-side. Again, the boundary-layer configuration resulting in the greatest difference in boundary-layer thickness from the wind to the lee-side results in the largest Magnus force.

In comparing the measured Magnus force coefficients obtained in this experiment to those published in Ref. 1, no agreement either in trend or magnitude is noted for the data at $M = 2$, $Re_l \approx 2 \times 10^6$. However, the data from Ref. 1 are in reasonable agreement with the data of this experiment for $M = 3$, $Re_l \approx 2 \times 10^6$. Close agreement for Magnus force between experiments conducted at different test facilities, especially at tunnel operating conditions which yield laminar or transitional boundary-layer configurations, should not be expected due to the extreme sensitivity of the Magnus force to boundary-layer configuration.

Reference

[1] Curry, W. H., Reed, J. F., and Ragsdale, W. C., "Magnus Data on the Standard 10° Cone Calibration Model," SC-DC 71 3821, March 1971, Sandia Labs., Albuquerque, N.Mex.

Drag Coefficients for Cones and Cylinders According to Schamberg's Model

MILDRED M. MOE*
Loyola University, Los Angeles, Calif.
AND
LOUIS C. TSANG†
Monsanto Company, St. Louis, Mo.

1. Introduction

THE earliest and simplest model of surface-particle interaction was proposed by Maxwell.[1] It has been used extensively

Received August 7, 1972; revision received September 28, 1972.
Index category: Rarefied Flows.
* Research Associate, Physics Department.
† Engineer, Corporate Engineering Department.